RSC
Medicinal Chemistry

ROYAL SOCIETY OF CHEMISTRY

RESEARCH ARTICLE

View Article Online
View Journal

Cite this: DOI: 10.1039/c9md00441f

Chromone and donepezil hybrids as new multipotent cholinesterase and monoamine oxidase inhibitors for the potential treatment of Alzheimer's disease†

Xiao-Bing Wang, Fu-Cheng Yin, Ming Huang, Neng Jiang, Jin-Shuai Lan and Ling-Yi Kong *

A series of chromone and donepezil hybrids were designed, synthesized, and evaluated as multipotent cholinesterase (ChE) and monoamine oxidase (MAO) inhibitors for the potential therapy of Alzheimer's disease (AD). *In vitro* studies showed that the great majority of these compounds exhibited potent inhibitory activity toward BuChE and AChE and clearly selective inhibition for *h*MAO-B. In particular, compound **5c** presented the most balanced potential for ChE inhibition (BuChE: IC_{50} = 5.24 μM; AChE: IC_{50} = 0.37 μM) and *h*MAO-B selectivity (IC_{50} = 0.272 μM, SI = 247). Molecular modeling and kinetic studies suggested that **5c** was a mixed-type inhibitor, binding simultaneously to peripheral and active sites of AChE. It was also a competitive inhibitor, which occupied the substrate and entrance cavities of MAO-B. Moreover, compound **5c** could penetrate the blood–brain barrier (BBB) and showed low toxicity to rat pheochromocytoma (PC12) cells. Altogether, these results indicated that compound **5c** might be a hopeful multitarget drug candidate with possible impact on Alzheimer's disease therapy.

Received 16th September 2019,
Accepted 8th November 2019

DOI: 10.1039/c9md00441f

rsc.li/medchem

1. Introduction

Alzheimer's disease (AD) is the most prominent form of dementia among the elderly that results in tremendous emotional and financial burden on society, individuals and their caregivers.[1] Data from 2018 indicated that approximately 50 million people around the world suffered from dementia, and the figure is going to increase sharply up to 132 million by 2050.[2] Although 100 years have passed since its discovery, the etiology of AD is still unclear. Many hypotheses have been developed to elucidate the molecular mechanism of AD based on several factors involved in its pathogenesis including β-amyloid (Aβ) deposits, τ-protein aggregation, oxidative stress, inflammation, dyshomeostasis of biometals and low levels of acetylcholine.[3]

Currently, the therapeutic treatments for AD are mainly focusing on the classical cholinergic hypothesis, which suggests that the low level of choline, especially ACh in the brain, is the key factor in its cognitive and memory deficits, and recovering or sustaining ACh can diminish these symptoms of AD.[4,5] It is rational and effective to increase the amount of ACh through inhibition of cholinesterases (ChEs) that are responsible for the hydrolysis of ACh in pre-synaptic areas for the treatment of AD's symptoms.[6] There are two types of ChEs in the central nervous system, butyrylcholinesterase (BuChE) and acetylcholinesterase (AChE). At present, several AChE inhibitors have been approved by the FAD for the treatment of AD including rivastigmine, donepezil, and galantamine. However, these single target drugs just have limited and transient impact on this disease in clinical therapy because of the multifactorial nature of AD.[7]

Many research studies have indicated that monoamine oxidase B (MAO-B) also played a pivotal role in the pathogenesis and development of AD. Its high level in the brain may cause a cascade of biochemical events, eventually leading to neuronal dysfunction.[8,9] Indeed, the age-related increase of brain MAO-B activity would produce higher levels of H_2O_2 and oxidative free radicals, which have been correlated with the development of oxidative stress.[10,11] On the other hand, recent biochemical and clinical studies indicated that MAO-B inhibitors, such as ladostigil and rasagiline, also have shown great antiapoptotic activities and neuroprotective and inhibitory effects on Aβ aggregation.[12–14] Thus, the development of MAO-B inhibitors has been considered as an attractive approach for the therapeutic strategy for AD.

Jiangsu Key Laboratory of Bioactive Natural Product Research and, State Key Laboratory of Natural Medicines, Department of Natural Medicinal Chemistry, School of Traditional Chinese Pharmacy, China Pharmaceutical University, 24 Tong Jia Xiang, Nanjing 210009, People's Republic of China.
E-mail: cpu_lykong@126.com; Fax: +86 25 83271405; Tel: +86 25 83271405

† Electronic supplementary information (ESI) available. See DOI: 10.1039/c9md00441f

In recent years, the multi-target-directed ligand (MTDL) strategy has shown a great advantage in the treatment of this multifaceted disease.[15–17] With the development of the "one molecule, multiple targets" paradigm, donepezil, which is the most effective pharmacological agent for AD treatment, has attracted more and more attention recently. A study of a donepezil–TcAChE complex by X-ray crystallography has revealed that donepezil is a dual binding site AChE inhibitor, and the indanone and benzylpiperidine moieties of donepezil could interact with the peripheral (non-catalytic) and central (catalytic) binding sites of AChE, respectively.[18] According to the MTDL strategy, it is advantageous to replace the indanone fragment of donepezil with additional bioactive molecules to produce multifunctional ChE inhibitors. For example, donepezil–ebselen hybrids have been designed as potent ChE inhibitors with various other ebselen-related pharmacological properties.[19] *N*-[(5-(Benzyloxy)-1-methyl-1*H*-indol-2-yl)methyl]-*N*-methylprop-2-yn-1-amine and donepezil hybrids have been designed as multifunctional agents capable of inhibiting MAOs and ChEs,[20] and a donepezil–RS67333 hybrid has been designed to be a dual serotonin subtype 4 receptor agonist/acetylcholinesterase inhibitor.[21] On the other hand, flavonoids, a large family of naturally occurring compounds, have been receiving increasingly widespread attention in present-day society because they exhibit a wide range of biological activities associated with neurological disorders especially for AD.[22,23] Indeed, several flavonoids have been shown to inhibit the development of AD and reverse cognitive deficits in rodent models, indicating that new effective flavonoid derivatives are promising candidates for the research on anti-AD drugs.[24–26] Recently, our group has reported the synthesis of tacrine–flavonoid and flavonoid–basic side-chain hybrids as multifunctional ChE inhibitors against AD.[27,28] Among them, the framework of chromone contributes greatly to the activities of flavonoid hybrids. The chromone (4*H*-1-benzopyran-4-one) structure is the pharmacophore of a great number of biologically active compounds. The ability to inhibit *h*MAO enzymes is one of the most developed method in AD research. The chromone core is found in flavones and isoflavones, which are molecules containing also the chalcone moiety; all these structures are preferential scaffolds for the development of *h*MAO inhibitors.[29]

In this paper, we are focused on studying chromone which has been recognized as a privileged scaffold for the development of monoamine oxidase inhibitors.[30,31] Considering that the combination of inhibitors targeting ChE and MAO-B is also an effective strategy for developing new multi-functional anti-AD drugs,[32–34] we combined chromone and the benzylpiperidine moieties of donepezil using an amide linker to obtain a series of new hybrids that are expected to be dual-acting AChE and MAO-B inhibitors (Fig. 1).

In this study, a series of new donepezil–chromone hybrids **4a–4h** and **5a–5h** were designed, synthesized and evaluated for their biological activity, including ChE and MAO inhibition as well as CNS permeation *in vitro*. Last, molecular modeling studies are performed to investigate the interaction mechanism, the structure–activity relationships and the binding mode of new hybrid compounds.

2. Results and discussion

2.1. Chemistry

Scheme 1 depicts the general procedure for the synthesis of donepezil–chromone hybrids **4a–4h** and **5a–5h**. 4-Oxo-4*H*-chromene-2-carboxylic acid (**3h**), 1-benzylpiperidin-4-amine (**4**) and 2-(1-benzylpiperidin-4-yl)ethanamine (**5**) are commercially available, whereas the 4-oxo-4*H*-chromene-3-carboxylic acids (**3a–3g**) were synthesized according to a described route.

Initially, 2-hydroxyacetophenones (**1a–1g**) were converted to 3-formylchromones (**2a–2g**) by a modified Harnisch procedure with phosphorus oxychloride and DMF. Then

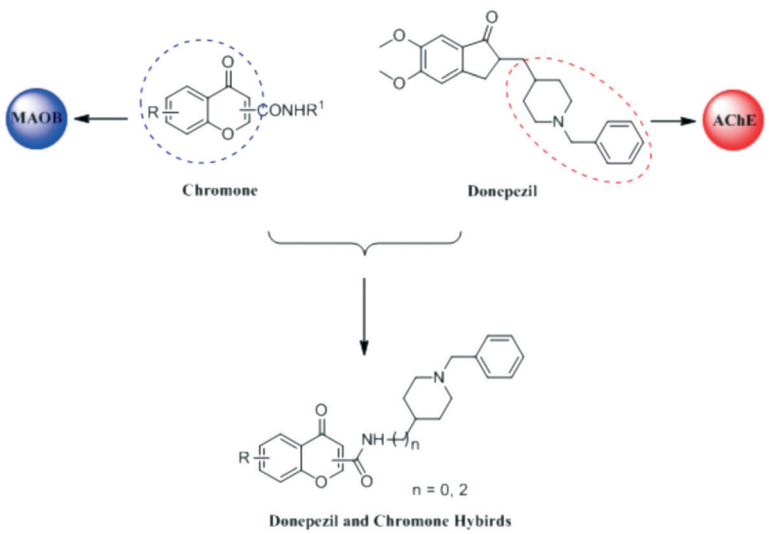

Fig. 1 Design strategy for donepezil and chromone hybrids.

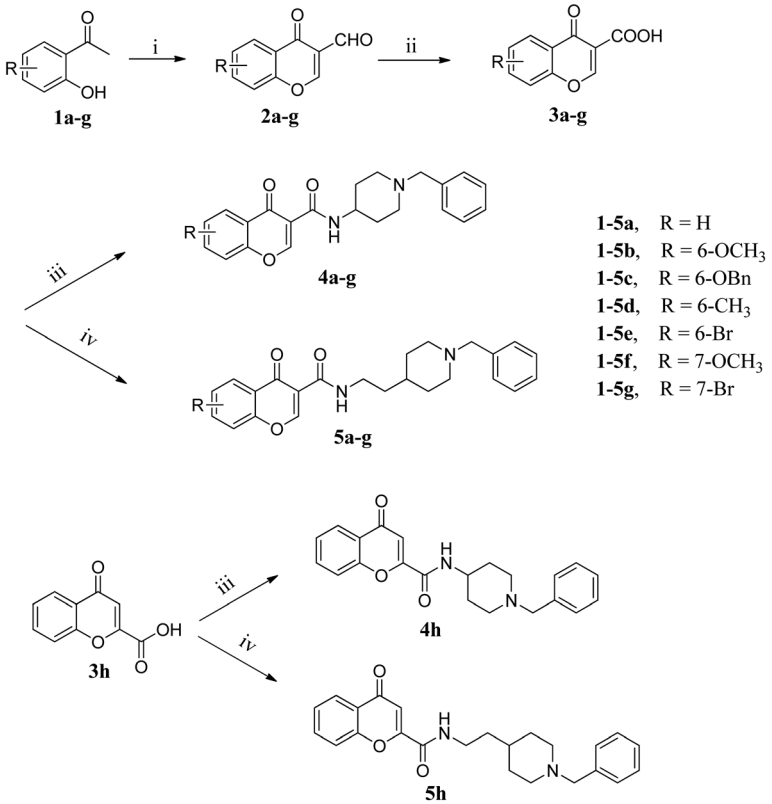

Scheme 1 Reagents and conditions: (i) $POCl_3$, DMF, 0 °C, 2 h; (ii) $NaClO_2$, NH_2HSO_3, CH_2Cl_2, 0 °C, 3 h; (iii) thionyl chloride, reflux; 1-benzylpiperidin-4-amine (**4**), K_2CO_3, CH_2Cl_2, rt, 8 h; (iv) thionyl chloride, reflux; 2-(1-benzylpiperidin-4-yl)ethanamine (**5**), K_2CO_3, CH_2Cl_2, rt, 8 h.

intermediates (**2a–2g**) were oxidized with sodium chlorite ($NaClO_2$) and sulfamic acid (NH_2SO_3H) to afford the corresponding acids (**3a–3g**).[35] Finally, **3a–3h** were treated with acetyl chloride and a catalytic amount of DMF in CH_2Cl_2 to produce the acyl chloride and subsequently reacted with 1-benzylpiperidin-4-amine (**4**) or 2-(1-benzylpiperidin-4-yl)ethanamine (**5**) in CH_2Cl_2, and the target compounds **4a–4h** and **5a–5h** were obtained in good yields.[36]

Table 1 Cholinesterases and human recombinant MAO isoforms inhibitory activity of tested compounds and reference compounds

Compd.	R	eeAChE IC_{50}[a] (μM)	eqBuChE IC_{50}[a] (μM)	Selectivity BuChE/AChE	*h*MAO-A inhibition[b] (%)	*h*MAO-B IC_{50}[a] (μM)	Selectivity *h*MAO-A/*h*MAO-B
4a	H	2.96 ± 0.22	18.67 ± 0.74	6.3	63.8 ± 5.7	17.68 ± 0.75	<5.6
4b	6-OCH_3	10.14 ± 0.54	24.36 ± 0.92	2.4	7.5 ± 0.7	46.27 ± 1.78	>2.1
4c	6-OBn	1.85 ± 0.16	12.43 ± 0.65	6.7	11.6 ± 0.5 μM[a]	0.035 ± 0.003	210.9
4d	6-CH_3	1.74 ± 0.14	15.27 ± 0.63	8.8	48.1 ± 2.7	19.46 ± 0.44	>5.1
4e	6-Br	1.57 ± 0.12	9.45 ± 0.82	6.1	35.5 ± 3.4	22.82 ± 0.74	>4.4
4f	7-OCH_3	1.58 ± 0.23	9.78 ± 0.86	6.2	37.4 ± 2.9	28.64 ± 0.68	>3.5
4g	7-Br	9.23 ± 0.65	18.24 ± 0.78	1.2	31.6 ± 2.5	19.73 ± 0.24	>5.1
4h	H	5.69 ± 0.43	27.86 ± 0.92	7.6	29.7 ± 2.2	33.29 ± 0.83	>3.1
5a	H	0.069 ± 0.03	0.60 ± 0.05	8.7	68.6 ± 6.7	35.29 ± 0.76	<2.8
5b	6-OCH_3	0.033 ± 0.02	0.45 ± 0.04	13.7	72.4 ± 8.4	11.23 ± 0.44	<8.9
5c	6-OBn	0.37 ± 0.05	5.24 ± 0.45	14.2	67.2 ± 0.7μM[a]	0.272 ± 0.04	247
5d	6-CH_3	0.11 ± 0.01	0.91 ± 0.07	8.3	30.6 ± 2.8	52.45 ± 1.68	>1.9
5e	6-Br	0.104 ± 0.09	1.17 ± 0.08	11.3	48.2 ± 4.5	26.13 ± 0.86	>3.8
5f	7-OCH_3	0.145 ± 0.08	0.52 ± 0.04	3.7	32.4 ± 2.7	30.93 ± 0.76	>3.2
5g	7-Br	0.154 ± 0.02	1.24 ± 0.07	11.9	30.3 ± 1.4	29.46 ± 0.82	>3.4
5h	H	0.31 ± 0.01	1.54 ± 0.12	4.9	29.5 ± 2.7	20.03 ± 0.24	>4.9
Donepezil	—	0.032 ± 0.02	2.47 ± 0.32	77	nt[c]	nt	—
Pargyline	—	nt.	nt.	—	nt.	0.12 ± 0.01	—
Iproniazid	—	nt.	nt.	—	5.89 ± 0.74 μM[a]	6.93 ± 0.34	0.85

[a] Data are the mean ± SD of three independent experiments. [b] Test concentration is 100 μM. [c] nt. = not tested.

2.2. Inhibitory activity against BuChE and AChE

The inhibitory activity of hybrids **4a–4h** and **5a–5h** against BuChE (from equine serum) and AChE (from electric eel) was evaluated with donepezil as the reference compound using Ellman's method.[37] The IC_{50} values and AChE selectivity ratios for inhibitory effects of all the test compounds are shown in Table 1. The results showed that all new target compounds showed moderate to good potent inhibitory activity to both ChEs with IC_{50} values ranging from micromolar to nanomolar. In particular, compound **5b**, with a 6-methoxy group substituent at the chromone moiety, provided the most potent inhibitory activity for ChEs (BuChE: IC_{50} = 0.45 μM, AChE: IC_{50}= 0.033 μM), quite similar to that obtained for donepezil (BuChE: IC_{50} = 2.47 μM, AChE: IC_{50} = 0.032 μM).

For the sake of clarity, all the hybrids were divided into two series according to the length of the carboxamide (compounds **4a–4h**) and *N*-ethylcarboxamide (compounds **5a–5h**) linkage. As seen in Table 1, the length of the linkage of the new compounds has great effects on the inhibitory activities of both AChE and BuChE. Generally, compounds **5a–5h** with *N*-ethylcarboxamide linkages between the benzylpiperidine and chromone manifest higher activity than their counterparts (**4a–4h**) with carboxamide linkages. On the other hand, the activity of chromones substituted at the 2-position (**4h** and **5h**) was slightly lower than those of the corresponding hybrids **4a** and **5a**. These results showed that the inhibitory potency against ChEs is also closely related to the position and length of the linkage.

In an effort to explore the effect of substitution at the benzene ring of the chromone moiety on the ChE inhibitory activities, we also have introduced different substituents with varying properties to chromone. From the IC_{50} values of compounds **5a–5e**, it appeared that the activity of substituent chromones against AChE was slightly less than that of corresponding non-substituted chromone **5a**. In particular, connecting the OCH_3 group to the 6-position of the chromone ring (**5b**) improves the inhibitory activity against AChE. Conversely, connecting the bulky OBn group to the 6-position (**5c**) led to a large reduction of efficacy against AChE isoforms. Moreover, compounds **5f** and **5g** possessing OCH_3 (**5f**) and Br (**5g**) groups at the 7-position of chromone showed a decreased AChE inhibitory activity compared to

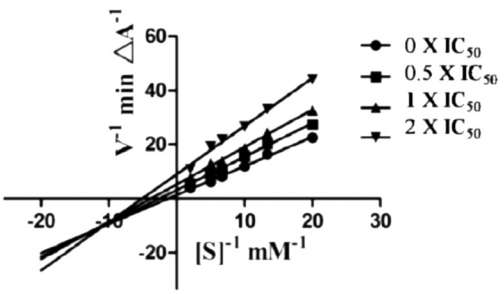

Fig. 2 Lineweaver–Burk plots resulting from the subvelocity curve of the AChE activity with different substrate concentrations (0.05–0.50 mM) in the absence and presence of 0.5 × IC_{50}, 1 × IC_{50}, and 2 × IC_{50} **5c**.

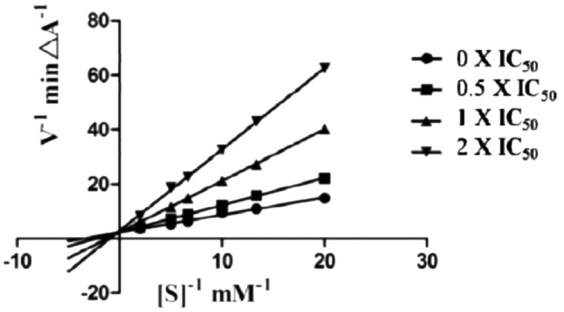

Fig. 3 Lineweaver–Burk plots resulting from the subvelocity curve of the BuChE activity with different substrate concentrations (0.05–0.50 mM) in the absence and presence of 0.5 × IC_{50}, 1 × IC_{50}, and 2 × IC_{50} **5c**.

the corresponding homologues **5b** and **5e** with the same substituent at the 6-position of chromone. These results indicated that both the steric hindrance and the electronic effects of the chromone enhance AChE inhibition. Interestingly, the opposite trend was observed for the effect of substituents on compounds **4a–4g**. For example, compound **4b** with 6-OCH_3 on the chromone exhibited the worst inhibitory activity, while compounds **4c–4f** with the other groups showed augmented AChE inhibitory activity.

In addition, the influence of the substitution at the benzene ring of the chromone moiety on BuChE inhibitory activity has the same trend as that on AChE inhibitory activity. Some evidence suggests that the inhibition of BuChE may also represent a treatment for Alzheimer's disease, with actions on memory and learning, possibly mediated through elevated ACh and lower Aβ levels.[38,39] Consequently, most of the hybrids exhibited good balanced AChE/BuChE inhibitory activity, and may represent good ChE inhibitors to treat Alzheimer's disease.

2.3. Inhibitory activity against *h*MAO-A and *h*MAO-B

To confirm the multipotent biological profile of the target compounds, inhibitory activity against MAOs was determined

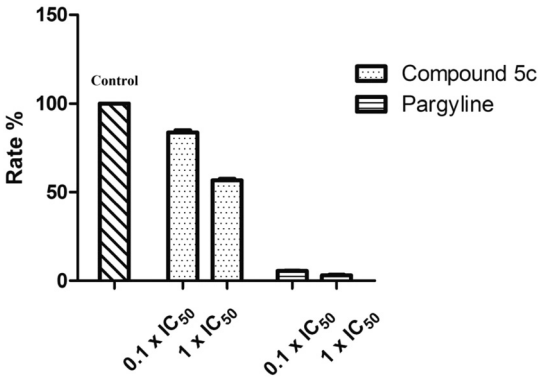

Fig. 4 Recovery of enzyme activity after dilution. MAO-B was pre-incubated with compounds **5c** and pargyline at concentrations equal to 10 × IC_{50} and 100 × IC_{50} for 30 min and then diluted to 0.1 × IC_{50} and 1 × IC_{50}, respectively. The residual enzyme activities were subsequently measured.

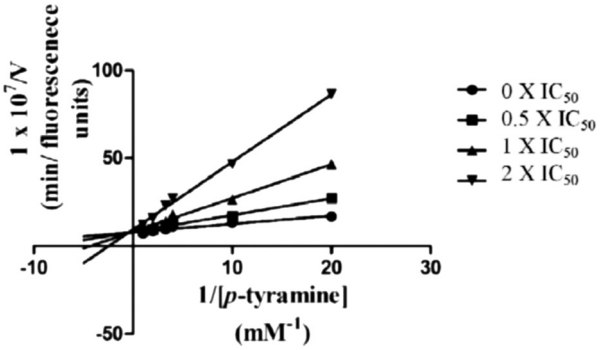

Fig. 5 Lineweaver–Burk plots resulting from the subvelocity curve of the MAO-B activity with different substrate concentrations (0.05–1.0 mM) in the absence and presence of 0.5 × IC_{50}, 1 × IC_{50}, and 2 × IC_{50} **5c**.

and compared with those of pargyline and iproniazid.[40] The results are depicted in Table 1. Most of these hybrids are moderate inhibitors of *h*MAO-B with IC_{50} values in the micromolar range, and exhibited weak or no inhibition of *h*MAO-A. A structure–activity relationship analysis showed that hybrids with the benzyloxy group at the 6 position of the chromone were favorable for inhibitory activity against *h*MAO-B. In particular, compound **4c**, featuring the benzyloxy group at the 6 position of the chromone, displayed the most potent inhibitory activity with an IC_{50} value of 0.035 μM, being about 3-fold and 200-fold more active than the references, pargyline (IC_{50} = 0.12 μM) and iproniazid (IC_{50} = 6.93 μM), respectively. All other analogues gave weaker activities when the benzyloxy group was substituted by other groups. Dramatically, compound **5d**, which featured a methyl group at the same position, provided the weakest. Moreover, MAO-B inhibitory potency was also closely related to the length of the alkylene chain. For example, compound **5c** with the *N*-ethylcarboxamide linkage between benzylpiperidine and chromone is also a great MAO-B inhibitor with an IC_{50} value of 0.272 μM, being about 7.8-fold less potent than its counterpart **4c** with a carboxamide linker. These results indicate that steric factors changed the *h*MAO-B inhibitory activity.

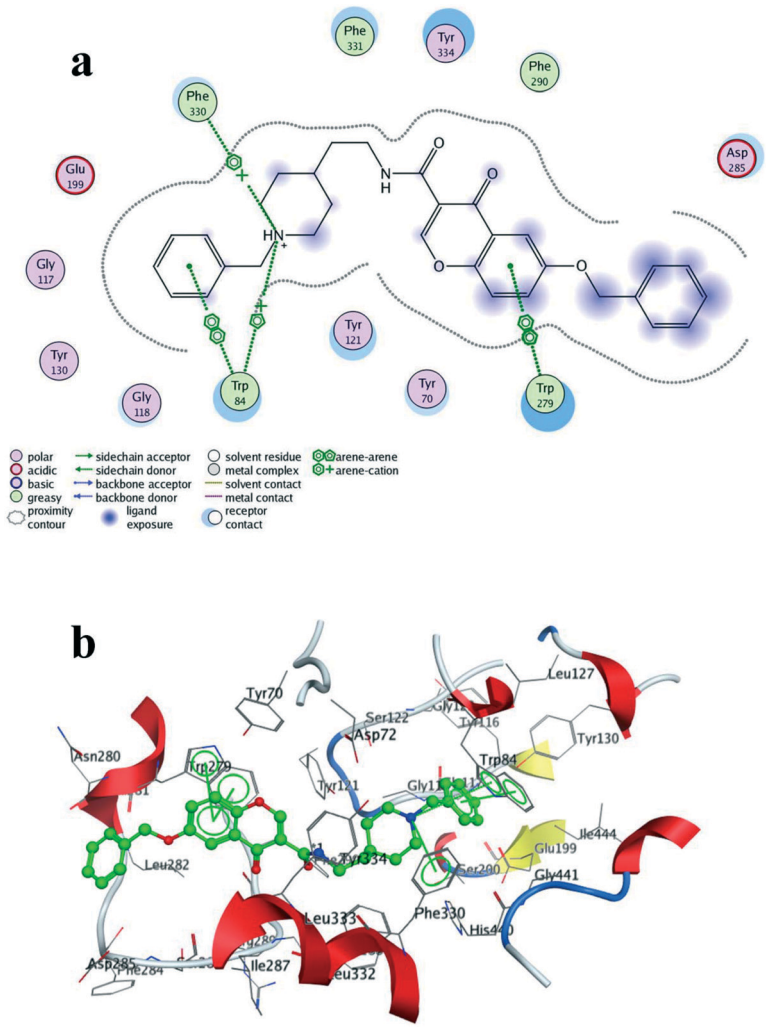

Fig. 6 Molecule docking of compound **5c** with AChE generated with MOE: (a) the 2D picture of binding is depicted; (b) the 3D picture of binding is depicted.

On account of the MAO and ChE inhibitory activity results, compound **5c**, which showed the most balanced potential to inhibit ChEs (AChE: IC_{50} = 0.37 μM; BuChE: IC_{50} = 5.24 μM) and MAO-B selectively (IC_{50} = 0.272 μM, SI = 247), is considered to be a promising multi-functional inhibitor for further study.

2.4. Kinetic studies for ChE

To gain information on the mechanism of action of compound **5c** on ChEs, kinetic studies were carried out. The Lineweaver–Burk reciprocal plots of **5c** against AChE (Fig. 2) showed increasing slopes and intercepts with higher inhibitor concentrations, indicating a mixed-type inhibitory behaviour for compound **5c** in the presence of AChE. Therefore this supports that compound **5c** could simultaneously bind to the PAS and CAS of AChE. In contrast, a different plot for BuChE was obtained, showing different K_m and constant V_{max} values in different inhibitor concentrations (Fig. 3). This suggested competitive inhibition, revealing that these compounds compete for the same binding site (CAS) as the substrate butyrylcholine.

2.5. Kinetic studies for *h*MAO-B

To study the inhibitory activity of **5c** toward *h*MAO-B, firstly, we analyzed the reversibility/irreversibility of the binding of compound **5c** by the recovery assay of the enzymatic activities after dilution of enzyme–inhibitor complexes.[41] Pargyline, with known irreversibility for *h*MAO-B, was used. The *h*MAO-B enzyme was firstly incubated with compound **5c** at concentrations of 10 × IC_{50} and 100 × IC_{50} for 30 min. These incubations were subsequently diluted 100-fold to yield inhibitor concentrations of 0.1 × IC_{50} and 1 × IC_{50}, respectively, and the residual enzyme catalytic rates were measured. In contrast to pargyline, we observed that **5c** reversibly inhibited MAO-B, since its MAO-B activities were recovered after diluting the enzyme–inhibitor complexes (Fig. 4). Then we have explored the possibility that **5c** acts as a competitive inhibitor of MAOB in accordance with a previous report.[30] For this purpose, the kinetic study of **5c** against *h*MAO-B was performed. As shown in Fig. 5, the Lineweaver–Burk plots for different concentrations of **5c** are linear and each set has a common *y*-intercept. This behaviour indicated that **5c** is a competitive

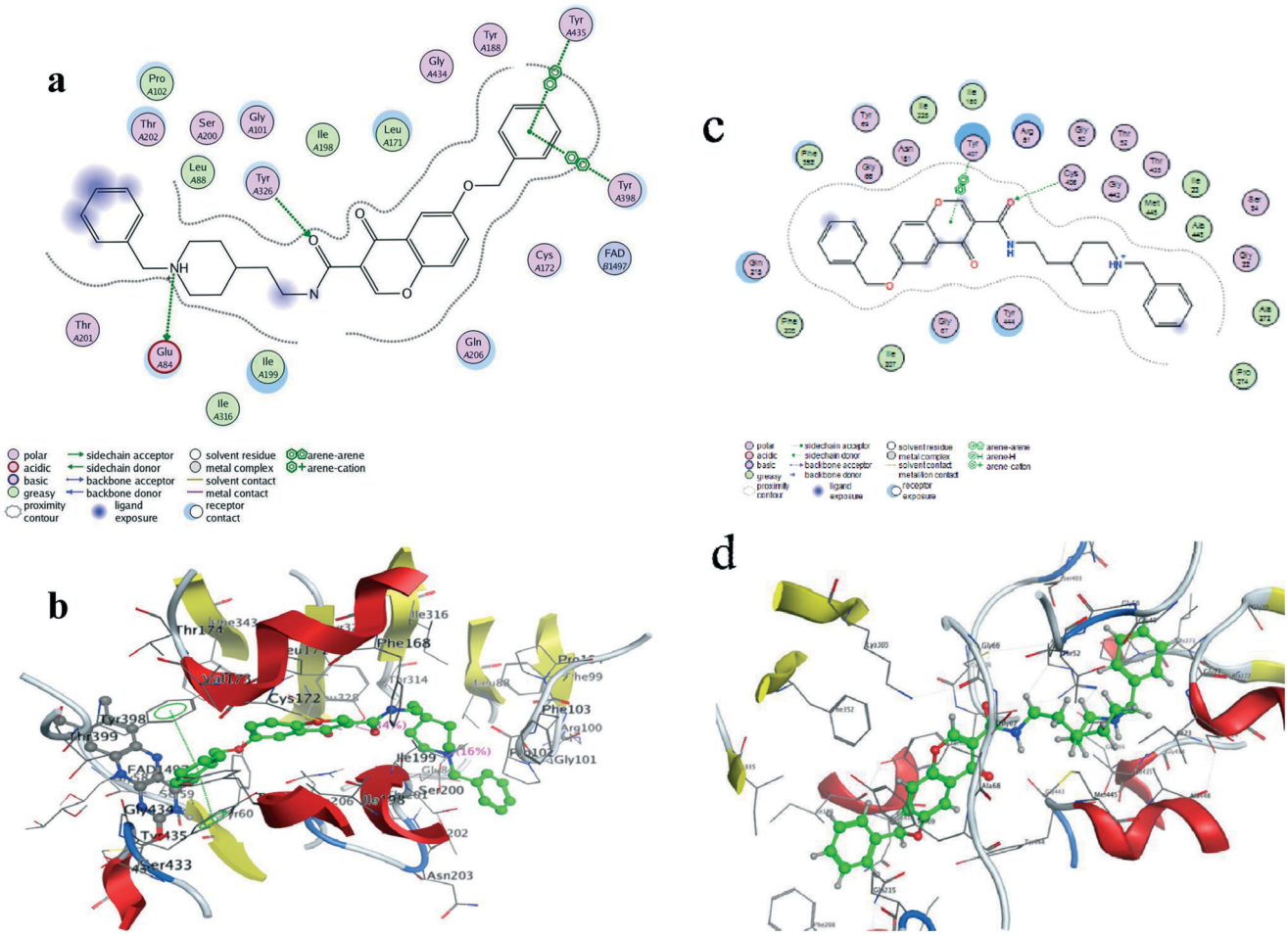

Fig. 7 Molecule docking of compound **5c** with MAO-B generated with MOE: (a) the 2D picture of binding is depicted; (b) the 3D picture of binding is depicted; (c) the 2D picture of binding of compound **5c** with MAO-A is depicted; (d) the 3D picture of binding of compound **5c** with MAO-A is depicted.

inhibitor of MAO-B isozymes and offers further support for the finding that **5c** is a reversible MAO-B inhibitor.

2.6. Molecular modeling studies of compound 5c with AChE

To obtain more insights into the interaction mode of compound **5c** against AChE, molecular docking study was performed using software package MOE 2008.10. The X-ray crystal structure of the *Tc*AChE complex with donepezil (PDB ID: 1EVE) was applied to build the starting model of AChE. As shown in Fig. 6, the *N*-benzylpiperidine moiety of **5c** was oriented towards the CAS of AChE, *via* π–cation interactions between the quaternary nitrogen of the piperidine ring with Trp84 and Phe330. Besides, its benzene ring could also interact with Trp84 *via* π–π stacking interactions. The chromone moiety interacted with the indole ring from Trp279 of the PAS *via* π–π stacking interactions. In addition, the 6-OBn of **5c** is exposed outside the active site of AChE, which may also, in part, explain the decreased inhibitory activity of AChE compared to that of **5a**. All these results clearly indicated that compound **5c** was a dual binding site (DBS) AChE inhibitor in agreement with the kinetic study, which demonstrated the rationality of our molecular design.

2.7. Molecular modeling studies for compound 5c with MAO-B and MAO-A

To evaluate the binding modes of the most potent compound **5c** with MAO-B and MAO-A, docking studies were employed with MOE 2008.10, based on the protein crystal structure of MAO-B (2V60) and MAO-A (2Z5Y). As can be seen from Fig. 7, the chromone moiety of **5c** is located within the substrate cavity of the enzyme, in close proximity of the flavin adenine dinucleotide (FAD) cofactor, and the π–π stacking interactions are seen between its benzyloxy group with Tyr435 and Tyr398. Meanwhile, Tyr326 is involved in a hydrogen bond interaction with the amide carbonyl of **5c**. In contrast, the benzylpiperidine moiety of **5c** occupies the hydrophobic pocket in the entrance cavity, formed by Pro102, Ser200, Leu88, Gly101, Thr201, Glu84, Ile199 and Ile316. Furthermore, a hydrogen bond was detected for the quaternary nitrogen of the piperidine ring with Glu84.

Table 2 Permeability ($P_e \times 10^{-6}$ cm s^{-1}) in the PAMPA-BBB assay for 9 commercial drugs, used in the experiment validation

Commercial drugs	Bibliography[a]	Experiment[b]
Testosterone	17	16.81 ± 1.23
Verapamil	16	21.01 ± 0.75
β-Estradiol	12	17.03 ± 0.44
Clonidine	5.3	8.14 ± 0.26
Corticosterone	5.1	3.11 ± 0.32
Piroxicam	2.5	1.32 ± 0.07
Hydrocortisone	1.9	1.41 ± 0.14
Lomefloxacin	1.1	1.81 ± 0.22
Ofloxacin	0.8	1.31 ± 0.01

[a] Taken from ref. 44. [b] Data are the mean ± SD of three independent experiments.

Table 3 Permeability results ($P_e \times 10^{-6}$ cm s^{-1}) from the PAMPA-BBB assay for selected compounds with their predicted penetration into the CNS

Compounds	Permeability[a] ($P_e \times 10^{-6}$ cm s^{-1})	Prediction
4a	15.6 ± 1.2	CNS+
4c	4.6 ± 0.6	CNS+
5b	16.7 ± 0.4	CNS+
5c	5.4 ± 0.3	CNS+

[a] Data are the mean ± SD of three independent experiments.

2.8. *In vitro* blood–brain barrier permeation assay

Since brain penetration is essential for successful anti-AD drugs,[42,43] we have evaluated the potential of these hybrids to cross the blood–brain barrier (BBB). For this purpose, a parallel artificial membrane permeation assay for BBB (PAMPA-BBB) was used, which was described by Di *et al.*[44] Assay validation was conducted by comparing experimental permeabilities of 9 commercial drugs with reported values (Table 2). A plot of experimental data *versus* bibliographic values gave a good linear correlation, P_e (exp.) = 1.2084 P_e (bibl.) − 0.3055 (R^2 = 0.9263). From this equation and considering the limit established by Di *et al.* for blood–brain barrier permeation, we established that compounds with permeability values over 4.5×10^{-6} cm s^{-1} should be able to cross the BBB. Four compounds (**4a**, **4c**, **5b** and **5c**) that exhibited good activity against AChE or MAO-B were chosen as the test compounds. The results summarised in Table 3 indicated that all of the selected hybrids (**4a**, **4c**, **5b** and **5c**) could penetrate the BBB to target the enzyme in the central nervous system.

2.9. Rat pheochromocytoma (PC12) cell toxicity

To gain insight into the therapeutic potential of these derivatives, the most potent compounds **4c**, **5b** and **5c** were selected as the candidates to further study the potential toxicity effect on the rat pheochromocytoma (PC12) cells (PC12 cells came from Cell Resource Center, Shanghai Institute of Life Sciences, Chinese Academy of Sciences). After exposing the cells to compounds **4c**, **5b** and **5c** for 24 h, cell viability was tested by the 3-(4,5-dimethylthiazol-2-yl)-2,5-diphenyltetrazolium (MTT) assay. As indicated in Fig. 8, these compounds did not

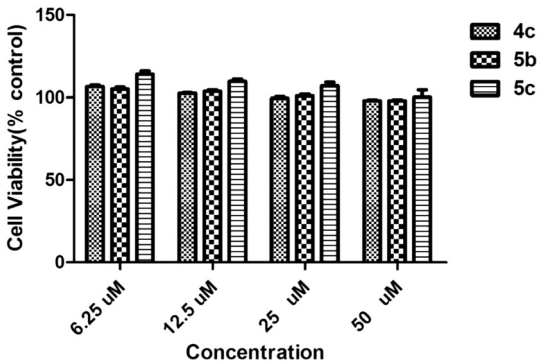

Fig. 8 The cell viability of compounds **4c**, **5b** and **5c** on PC12 cells at 0–50 μM.

show significant effects on cell viability at 1–50 μM. This suggested that compounds **4c**, **5b** and **5c** were nontoxic to PC12 cells and might be suitable multifunctional agents for treating AD.

3. Conclusion

In summary, a series of donepezil and chromone hybrids have been designed, synthesized and evaluated as multi-functional anti-AD agents with cholinesterase and MAO inhibitory activities. Most of the compounds were potent ChE inhibitors with IC_{50} values ranging from micromolar to nanomolar. These hybrids were also potent, exhibited high MAO-B selectivity and interacted reversibly with *h*MAO-B. Among the synthesized compounds, compound **5c** was the most attractive derivative, being able to inhibit ChEs (AChE: IC_{50} = 0.37 μM; BuChE: IC_{50} = 5.24 μM) and having high MAO-B selectivity (IC_{50} = 0.272 μM, SI = 247). Meanwhile, compound **5c** could penetrate the blood–brain barrier (BBB) and showed low cell toxicity to rat pheochromocytoma (PC12) cells *in vitro*. Altogether, the multifunctional ligand **5c** endowed with balanced inhibitory activities for ChEs and MAO-B might be considered as a promising anti-AD candidate for further research.

Conflicts of interest

There are no conflicts of interest to declare.

Acknowledgements

This research work was financially supported by the National Natural Science Foundation of China (81573313), the Innovative Research Team in University (IRT_15R63), a project funded by the Priority Academic Program Development of Jiangsu Higher Education Institutions (PAPD), and the Project of Graduate Education Innovation of Jiangsu Province (No. CXZZ13_0320).

References

1 D. M. Walsh and D. J. Selkoe, *Neuron*, 2004, **44**, 181–193.
2 *World Alzheimer Report 2018 | Alzheimer's Disease International*, https://www.alz.co.uk/research/world-report-2018.
3 P. Schelterns and H. Feldman, *Lancet Neurol.*, 2003, **2**, 539–547.
4 V. N. Talesa, *Mech. Ageing Dev.*, 2001, **122**, 1961–1969.
5 Q. Xie, H. Wang, Z. Xia, M. Lu, W. Zhang, X. Wang, W. Fu, Y. Tang, W. Sheng and W. Li, *J. Med. Chem.*, 2008, **51**, 2027–2036.
6 E. Giacobini, *Pharmacol. Res.*, 2004, **50**, 433–440.
7 G. Pepeu and M. G. Giovannini, *Curr. Alzheimer Res.*, 2009, **6**, 86–96.
8 J. Shih, K. Chen and M. Ridd, *Annu. Rev. Neurosci.*, 1999, **22**, 197.
9 G. D. Mellick, D. D. Buchanan, S. J. McCann, K. M. James, A. G. Johnson, D. R. Davis, N. Liyou, D. Chan and D. G. Le Couteur, *Mov. Disord.*, 1999, **14**, 219–224.
10 J. Saura, J. Luque, A. Cesura, M. D. Prada, V. Chan-Palay, G. Huber and J. Löffler, *J. Neurosci.*, 1994, **62**, 15–30.
11 M. Nebbioso, A. Pascarella, C. Cavallotti and N. Pescosolido, *Int. J. Exp. Pathol.*, 2012, **93**, 401–405.
12 M. Yogev-Falach, O. Bar-Am, T. Amit, O. Weinreb and M. B. Youdim, *FASEB J.*, 2006, **20**, 2177–2179.
13 M. B. Youdim and M. Weinstock, *Cell. Mol. Neurobiol.*, 2001, **21**, 555–573.
14 O. Bar-Am, T. Amit, O. Weinreb, M. B. Youdim and S. Mandel, *J. Alzheimer's Dis.*, 2010, **21**, 361–371.
15 B. Kumar, V. Kumar, V. Prashar, S. Saini, A. R. Dwivedi, B. Bajaj, D. Mehta, J. Parkash and V. Kumar, *ACS Chem. Neurosci.*, 2019, **10**, 252–265.
16 B. Kumar, A. R. Dwivedi, B. Sarkar, S. K. Gupta, S. Krishnamurthy, A. K. Mantha, J. Parkash and V. Kumar, *Eur. J. Med. Chem.*, 2019, **177**, 221–234.
17 A. Cavalli, M. L. Bolognesi, A. Minarini, M. Rosini, V. Tumiatti, M. Recanatini and C. Melchiorre, *J. Med. Chem.*, 2008, **51**, 347–372.
18 G. Kryger, I. Silman and J. L. Sussman, *Structure*, 1999, **7**, 297–307.
19 Z. Luo, J. Sheng, Y. Sun, C. Lu, J. Yan, A. Liu, H. B. Luo, L. Huang and X. Li, *J. Med. Chem.*, 2013, **56**, 9089–9099.
20 I. Bolea, J. Juarez-Jimenez, C. de Los Rios, M. Chioua, R. Pouplana, F. J. Luque, M. Unzeta, J. Marco-Contelles and A. Samadi, *J. Med. Chem.*, 2011, **54**, 8251–8270.
21 C. Lecoutey, D. Hedou, T. Freret, P. Giannoni, F. Gaven, M. Since, V. Bouet, C. Ballandonne, S. Corvaisier, A. Malzert Freon, S. Mignani, T. Cresteil, M. Boulouard, S. Claeysen, C. Rochais and P. Dallemagne, *Proc. Natl. Acad. Sci. U. S. A.*, 2014, **111**, 3825–3830.
22 F. I. Baptista, A. G. Henriques, A. M. Silva, J. Wiltfang and O. A. da Cruz e Silva, *ACS Chem. Neurosci.*, 2014, **5**, 83–92.
23 X. He, H. M. Park, S. J. Hyung, A. S. DeToma, C. Kim, B. T. Ruotolo and M. H. Lim, *Dalton Trans.*, 2012, **41**, 6558–6566.
24 D. Vauzour, *J. Sci. Food Agric.*, 2014, **94**, 1042–1056.
25 A. Nakajima, Y. Ohizumi and K. Yamada, *Clin. Psychopharmacol. Neurosci.*, 2014, **12**, 75–82.
26 A. M. Haque, M. Hashimoto, M. Katakura, Y. Tanabe, Y. Hara and O. Shido, *J. Nutr.*, 2006, **136**, 1043–1047.
27 S. Y. Li, X. B. Wang, S. S. Xie, N. Jiang, K. D. Wang, H. Q. Yao, H. B. Sun and L. Y. Kong, *Eur. J. Med. Chem.*, 2013, **69**, 632–646.
28 R. S. Li, X. B. Wang, X. J. Hu and L. Y. Kong, *Bioorg. Med. Chem. Lett.*, 2013, **23**, 2636–2641.
29 P. Guglielmi, S. Carradori, A. Ammazzalorso and D. Secci, *Expert Opin. Drug Discovery*, 2019, **14**, 995–1035.
30 L. J. Legoabe, A. Petzer and J. P. Petzer, *Eur. J. Med. Chem.*, 2012, **49**, 343–353.
31 A. Gaspar, F. Teixeira, E. Uriarte, N. Milhazes, A. Melo, M. N. Cordeiro, F. Ortuso, S. Alcaro and F. Borges, *ChemMedChem*, 2011, **6**, 628–632.
32 L. Bica, P. J. Crouch, R. Cappai and A. R. White, *Mol. BioSyst.*, 2009, **5**, 134–142.
33 O. M. Bautista-Aguilera, G. Esteban, M. Chioua, K. Nikolic, D. Agbaba, I. Moraleda, I. Iriepa, E. Soriano, A. Samadi, M.

Unzeta and J. Marco-Contelles, *Drug Des., Dev. Ther.*, 2014, **8**, 1893–1910.

34 O. M. Bautista-Aguilera, G. Esteban, I. Bolea, K. Nikolic, D. Agbaba, I. Moraleda, I. Iriepa, A. Samadi, E. Soriano, M. Unzeta and J. Marco-Contelles, *Eur. J. Med. Chem.*, 2014, **75**, 82–95.

35 L. J. Legoabe, A. Petzer and J. P. Petzer, *Bioorg. Med. Chem. Lett.*, 2012, **22**, 5480–5484.

36 S. Y. Li, N. Jiang, S. S. Xie, K. D. Wang, X. B. Wang and L. Y. Kong, *Org. Biomol. Chem.*, 2014, **12**, 801–814.

37 G. L. Ellman, K. D. Courtney, V. Andres Jr. and R. M. Feather-Stone, *Biochem. Pharmacol.*, 1961, **7**, 88–95.

38 N. H. Greig, T. Utsuki, D. K. Ingram, Y. Wang, G. Pepeu, C. Scali, Q. S. Yu, J. Mamczarz, H. W. Holloway, T. Giordano, D. Chen, K. Furukawa, K. Sambamurti, A. Brossi and D. K. Lahiri, *Proc. Natl. Acad. Sci. U. S. A.*, 2005, **102**, 17213–17218.

39 B. Brus, U. Košak, S. Turk, A. Pišlar, N. Coquelle, J. Kos, J. Stojan, J. P. Colletier and S. Gobec, *J. Med. Chem.*, 2014, **57**, 8167–8179.

40 L. Santana, H. González-Díaz, E. Quezada, E. Uriarte, M. Yáñez, D. Viña and F. Orallo, *J. Med. Chem.*, 2008, **51**, 6740–6751.

41 L. J. Legoabea, A. Petzera and J. P. Petzer, *Bioorg. Chem.*, 2012, **45**, 1–11.

42 W. M. Pardridge, *Alzheimer's Dementia*, 2009, **5**, 427–432.

43 V. Hachinski and T. Y. Lee, *Alzheimer's Dementia*, 2009, **5**, 435–436.

44 L. Di, E. H. Kerns, K. Fan, O. J. McConnell and G. T. Carter, *Eur. J. Med. Chem.*, 2003, **38**, 223–232.